RESEARCH

CNS Neuroscience & Therapeutics

# Effects of Acetazolamide on Transient $K^+$ Currents and Action Potentials in Nodose Ganglion Neurons of Adult Rats

Shigeji Matsumoto,[1] Shinki Yoshida,[1] Mizuho Ikeda,[1] Jun Kadoi,[1] Masayuki Takahashi,[1] Takeshi Tanimoto,[1] Junichi Kitagawa,[2] Chikako Saiki,[1] Mamoru Takeda[1] & Yukio Shima[3]

1 Department of Physiology, Nippon Dental University, School of Life Dentistry at Tokyo, 1-9-20 Fujimi, Chiyoda-ku, Tokyo 102-8159, Japan
2 Department of Physiology, Nihon University, School of Dentistry, 1-8-13, Kanda-Surugadai, Chiyoda-ku, Tokyo 101-8310, Japan
3 Laboratory of Biochemistry, Kyorin University, School of Health Sciences, 476 Miyashita-Cho, Hachioji City, Tokyo 192-8508, Japan

**Keywords**
Acetazolamide; Carbonic anhydrase; 4-aminoprydine; Immunoreactivity; Neuronal activity; Nodose ganglion; Voltage-dependent $K^+$ channel protein.

**Correspondence**
Shigeji Matsumoto, D.D.S., Ph.D., Department of Physiology, Nippon Dental University, School of Life Dentistry at Tokyo, 1-9-20 Fujimi, Chiyoda-ku, Tokyo 102-8159, Japan.
Tel.: +81-3-3261-8706;
Fax: +81-2-3261-8740;
E-mail: matsu-s@tky.ndu.ac.jp

doi: 10.1111/j.1755-5949.2010.00133.x



The aim of the present study was to determine whether acetazolamide (AZ) contributes to the inhibition of the fast inactivating transient $K^+$ current ($I_A$) in adult rat nodose ganglion (NG) neurons. We have previously shown that pretreatment with either AZ or 4-AP attenuated or blocked the $CO_2$-induced inhibition of slowly adapting pulmonary stretch receptors in *in vivo* experiments. The patch-clamp experiments were performed by using the isolated NG neurons. In addition to this, the RT-PCR of mRNA and the expression of voltage-gated $K^+$ (Kv) 1.4, Kv 4.1, Kv 4.2, and Kv 4.3 channel proteins from nodose ganglia were examined. We used NG neurons sensitive to the 1 mM AZ application. The application of 1 mM AZ inhibited the $I_A$ by approximately 27% and the additional application of 4-AP (1 mM) further inhibited $I_A$ by 48%. The application of 0.1 $\mu$M $\alpha$-dendrotoxin ($\alpha$-DTX), a slow inactivating transient $K^+$ current ($I_D$) blocker, inhibited the baseline $I_A$ by approximately 27%, and the additional application of 1 mM AZ further decreased the $I_A$ by 51%. In current clamp experiments, AZ application (1 mM) increased the number of action potentials due to the decreased duration of the depolarizing phase of action potentials and/or due to a reduction in the resting membrane potential. Four voltage-gated $K^+$ channel proteins were present, and most (80–90%) of the four Kv channels immunoreactive neurons showed the co-expression of carbonic anhydrase-II (CA-II) immunoreactivity. These results indicate that the application of AZ causes the reduction in $I_A$ via the inhibition of four voltage-gated $K^+$ channel (Kv) proteins without affecting $I_D$.

## Introduction

Enzymatic dispersion of the ganglia separates the neuronal soma from its axons, and as a result, the patch-clamp study has been used to investigate the electrophysiological properties of neurons without intact afferent fibers. Nodose ganglia neurons innervate a variety of tissues including the pulmonary, cardiovascular, and gastrointestinal afferent inputs. In conventional intracellular recording techniques using NG neurons, 90% of them have unmyelinated axons and the remaining neurons have myelinated axons [1,2]. Based on the analysis of neurons possessing the conduction velocity (CV, m/s) and action potential (AC) duration (ms) by using slices of nodose ganglia with intact vagal axons, Li and Schild [3] identified two types of myelinated afferent fibers: one group (10/76, 13%) exhibited CVs in excess of 10 m/s with narrow (<1 ms) AC duration while the another group (9/76, 12%) had CVs as low as 4 m/s with broad AC (>2 ms), and the remaining neurons (57/75, 75%) were identified as unmyelinated afferent fibers with either CVs less than 1 m/s or an AC duration of over 2 ms. The SARs are known to be mechanoreceptors that slowly adapt to a varying mechanical stimulus. It has been reported that the $CO_2$-induced inhibition of SARs is blocked or attenuated by the administration of either

acetazolamide (AZ), a carbonic anhydrase inhibitor, or 4-AP (a $K^+$ channel blocker) in *in vivo* experiments using rabbits [4,5] and rats [6,7]. When considering these results, taken together, it seems likely that NG neurons responding to AZ may be useful to investigate the physiological properties of the soma of SARs.

There are many observations on the electrophysiological properties of NG neurons [8–11]. For example, several voltage-gated $K^+$ (Kv) channels have the ability to regulate the action potential shape, adaptation, and excitability of sensory neurons. The fast inactivating $K^+$ (A-type) current ($I_A$) in NG is known to be inhibited by the application of 4-AP at the concentration range of 1 to 30 $\mu$M [12]. Such a current is also involved in a slow inactivating transient $K^+$ current ($I_D$) sensitive to lower concentrations of $\alpha$-dendrotoxin ($\alpha$-DTX) and 4-AP [13–15]. Furthermore, there is a report stating that after the loss of $I_D$ due to 0.1 $\mu$M $\alpha$-DTX application, the additional application of 0.5 mM 4-AP still modulates the properties of the action potential number and shape in adult rat small-diameter trigeminal ganglion (TG) neurons, indicating that the $I_D$ is a component of the $I_A$ [16]. In the isolated guinea-pig trachea/bronchus preparation using NG-derived vagal afferent fiber having mechanically sensitive receptive fields, the application of either 1 mM 4-AP or 1 $\mu$M $\alpha$-DTX could elicit spontaneous action potentials but neither tetraethylammonium (TEA), iberiotoxin, glybenclamide, 5,8,11,14-eicosatetreyonic acid (ETYA), BDS-II, nor apamin caused action potential generation [17]. In addition, there are no reports to examine whether AZ influences 4-AP-sensitive $K^+$ currents involving $I_A$ and/or $I_D$ in adult rat NG neurons. There is evidence that the elctrophysiological properties of the membranes of soma in primary afferent neurons are similar to those of peripheral terminals in the same neurons [18].

The purposes of the present study were designed to evaluate to what extent AZ inhibits $I_A$ without and with the loss of $I_D$ and how the responses of action potential properties are altered by the application of AZ before and after pretreatment with 4-AP in adult rat NG neurons. To determine whether homogenetic Kv 1.4 channels are predominant on NG neurons, the expression of A-type $K^+$ channel proteins such as Kv 1.4 and the Kv 4 family (Kv 4.1, Kv 4.2, and Kv 4.3) was examined by means of reverse transcription–polymerase chain reaction (RT-PCR) analysis. Furthermore, we also examined whether CA-II-immunoreactive cells are actually co-expressed in NG neurons that express immunoreactivities for Kv 1.4 and the Kv 4 family (Kv 4.1–4.3). Our data support the idea that the reduced $I_A$ following the 1 mM AZ application would occur as a result of the combined inhibition of Kv 1.4 and Kv 4.1–4.3 channels.

## Materials and Methods

All animal studies were approved by the *Guide for the Care and Use of Laboratory Animals* published by the U.S. National Institutes of Health (NIH Publication No. 85–23, revised 1996). In addition, all experimental protocols used in this study were approved by the Animal Use and Care Committee of Nippon Dental University. We minimized the number of animals used and their suffering.

### Cell Culture

Primary cultures of dissociated adult male rat NG neurons were prepared as described previously [18–21]. Wistar rats (200–300 g) were deeply anesthetized with pentobarbital sodium (50–60 mg/kg, i.p.). The nodose ganglia were identified, dissected from the vagus nerve trunks and placed in modified Hank's balanced solution (HBSS) containing (in mM) 130 NaCl, 5 KCl, 0.3 $KH_2PO_4$, 4 $NaHCO_3$, 0.3 $Na_2HPO_4$, 5.6 glucose, and 10 HEPES. The dissected nodose ganglia were transferred to HBSS containing collagenase types XI (1.5 mg/mL: Sigma-Aldrich, St. Louis, MD, USA) and II (1.5 mg/mL, Sigma-Aldrich). The cells were triturated with a fire-polished Pasteur pipette and subsequently were plated onto the cover slips pretreated with Poly-L-lysine in a 35-mm dish. The planting medium contained a Leibovitz's L-15 solution (Invitrogen Corp., Carlsbad, CA, USA) supplemented with 10% newborn calf serum, 50 U/mL penicillin-streptomycin (Invitrogen Corp.), 26 mM $NaHCO_3$, and 10 mM glucose. The cells were recorded within 2 to 10 h following plating. Neurons were accepted for study only if they showed a stable resting membrane potential exceeding −45 mV and an action potential overshoot of more than +30 mV.

### Electrophysiology

Whole-cell patch-clamp recordings were performed at room temperature (22–25°C). The current was measured with an amplifier (Axopatch-1D; Axon Instruments Inc., Union City, CA, USA). The pipette resistance was 2 to 4 MΩ. After the pipette was filled with a recording solution, currents and voltages were low-pass filtered at 5 to 10 kHz with a four-pole Bessel filter and digitally sampled at 25 to 100 kHz. After seal formation and membrane disruption, capacity transients (31–38 pF) were cancelled. The electrode access resistance (7–10 MΩ) also showed compensations within 80–90%. Data obtained from the neurons in which uncompensated series resistance resulted in voltage-clamp errors of >5 mV did not undergo any further analysis. No corrections were made for liquid junction potentials before recording and this

potential was calculated to be 6 mV. The whole-cell leak current produced by the 10 mV depolarizing step pulse was normally less than 10 pA. Isolated cells on a glass cover slip dish were placed in a recording chamber (volume, 0.5 mL) and visualized under the phase contrast of an inverted microscope (Nikon, Tokyo, Japan). The chamber was perfused under gravity with a standard external solution of approximately 0.5 mL/min. The drugs dissolved into the external solution were administered via a linear array of seven super fusion polyethylene tubes (280 $\mu$m in diameter) positioned close to the cell bodies (approximately 200 $\mu$m).

## I-Clamp

Current injections for 300 ms were applied in increments of 50 pA. Action potentials were initially evoked by a depolarizing pulse at one threshold (1 T); the action potential number was measured during 3 times T (3 T). We classified NG neurons as slowly adapting (SA)-type NG neurons, as described in previous studies [22–24]. During current injection at 3T, we determined whether AZ has 4-AP-like effects on the action potential in NG neurons showing multiple action potentials of more than two spikes. In some experiments, changes in action potential characteristics [firing frequency, resting membrane potential (RMP), duration of half-amplitude of action potential, duration of the depolarization phase of the action potential (DDP), duration of the repolarization phase of the action potential (DRP)] in response to current injections at 3 T were examined before and after the application of AZ or 4-AP as well as during their combined applications.

## V-Clamp

The $K^+$ currents were recorded from NG neurons (soma diameter <35 $\mu$m). We further distinguished a transient $K^+$ current ($I_A$) from a sustained $K^+$ current ($I_K$) and the total outward $K^+$ current by using the same steps described in previous studies [11,16,17,25–27]. Outward $K^+$ currents were identified by applying a conditioning pulse of either −40 or −120 mV from a holding potential of −80 mV; then, the membrane was depolarized from −40 or −120 mV to +60 mV in increments of 10 mV, and +60 mV produced the largest peak in each recording. The $I_A$ was determined by subtracting the −40 mV protocol from the −120 mV protocol. Activation of the currents was rapid and only partially delayed during the 200-ms depolarization pulse. In some experiments, 4-AP, $\alpha$-DTX, and AZ were used to determine whether AZ has 4-AP-like effects on $K^+$ currents. Before recordings the $K^+$ currents, we initially confirmed that the NG neurons used in this study were sensitive to 1 mM AZ application, by using I-clamp techniques as described above. In order to measure the $K^+$ currents, replacement of the external solution was performed for 7–8 min.

## Solutions

The external solution for the current clamp experiment of the action potential contained 160 mM NaCl, 5 mM KCl, 10 mM HEPES, 1 mM $MgCl_2$, 2 mM $CaCl_2$, and 10 mM glucose; pH adjusted to 7.4 with NaOH. The internal solution contained 140 mM KCl, 10 mM HEPES, 10 mM EGTA, 1 mM $CaCl_2$, 2 mM Mg-ATP, and 14 mM $Na_2$ creatine phosphate; the pH was adjusted to 7.3 with KOH. For the voltage clamp experiment of the voltage-dependent $K^+$ current, the external solution contained 160 mM N-methyl D-glucamine (NMDG), 5 mM KCl, 10 mM HEPES, 1 mM $MgCl_2$, and 10 mM glucose; the pH was adjusted to 7.4 with KOH, and the internal solution was the same as that used for the current clamp experiments. The estimation of the free $Ca^{2+}$ concentration ranged from 10 to 100 nM in the internal solution that had both EGTA (10 mM) and $CaCl_2$ (1 mM). That concentration was the normal $Ca^{2+}$ for sensory neurons. Under such conditions of EGTA and $CaCl_2$, voltage-gated $Ca^{2+}$ currents were successfully recorded in small-diameter TG neurons from neonatal rats [28].

## Drugs

All drugs (stock solutions) were stored at −20°C and dissolved in the external solution. AZ (Sanwa Kagaku Kenkyusho Co. Ltd., Nagoya, Japan, 500 mg) was diluted with 0.9% NaCl solution (20 mg/mL). AZ, a CA inhibitor (0.01–10 mM), 4-AP, an $I_A$ blocker (1 mM; Sigma-Aldrich); and $\alpha$-DTX, an $I_D$ blocker (0.1 $\mu$M, Alomone Labs, Jerusalem, Israel) were added to the perfusion. Maren et al. [29] demonstrated that concentrations greater than $10^{-4}$ M, corresponding to 20 mg/kg in *in vivo* experiments, have a nonspecific effect. We used 1 mM AZ, which is nearly equal to the calculated value (20 mg/kg), as used in *in vivo* experiments. The molecular weight for AZ is 222.25 g. Assuming the total blood volume of a rat is about 6.5 mL/100 g [30] would be between 13 and 19.5 mL of total blood diluting 4–6 mg per 200–300 g rat, respectively. These calculations are that 20 mg/kg of AZ would be closer to 1.3 mM. Therefore, we examined lower and higher concentrations of 1 mM AZ.

## Statistical Analysis

In voltage clamp experiments, the effects of test agents (4-AP, 4-AP+AZ, $\alpha$-DTX, and $\alpha$-DTX+AZ) were calculated as the changes in the current density–voltage curve. In current clamp experiments, the changes in the action potential properties were examined before and after AZ in the absence and presence of 4-AP. Statistical analyses of physiological studies were performed using a paired *t*-test and/or a repeated measure ANOVA with Tukey's *post hoc* test for paired samples. In addition, the group comparisons of mean values (4-AP only vs. AZ+4-AP; $\alpha$-DTX only vs. $\alpha$-DTX+AZ) were performed using Student's unpaired *t*-test. *P* values of less than 0.05 were considered statistically significant.

## Kv Channel Protein

Total RNA was isolated from the whole nodose ganglia of six adult rats (240–300 g) with a Perfect RNA Eukaryotic kit (Expender, Germany) as described in a previous study [31]. Total RNA was treated with DNase I (Invitrogen Corp.) at room temperature for 15 min to remove any contaminating genomic DNA. The enzyme was removed by a phenol-chloroform extraction. With the use of the optical density reading, the total RNA purification was confirmed to yield an A260 $A280^{-1}$ ratio of 1.9–2.0. The RT-PCR was conducted with the RT Applied Biosystems Kit (Applied Biosystems, Chiba, Japan). The primers used for the Kv 1.4, Kv 4.1–4.3, and GAPDH were 5′-GAAAACGAACAGACCCAGC-3′ and 5′-ATACTCTGACTTGTCCCCCAGG-3′, 5′-CGGACAAATGC TGTGCGTTAG-3′ and 5′-TAGGGGAGAGGAAGTTGACT TTCAT-3′, 5′-AACGAGCG-ACAAAGGAAG-3′ and 5′-TCAGTAACCCATTCCGCTTG-3′, 5′-TGACAACACTG GGGTATGGA-3′ and 5′-AACAGGGGATCATCCACAAG-3′, and 5′-CGGAGTCAACGGATTTGGTCGTAT-3′ and 5′-AGCCTTCTCCATGGTGGTGAAGAC-3′, respectively. A total 10 $\mu$L reaction volume containing 200 ng of total RNA, 1 $\mu$L of RT reaction solution, 0.4 $\mu$M of each primer, 200 $\mu$M each dNTP, 1.5 mM $MgCl_2$, 50 mM KCl, 10 mM Tris-HCl (pH = 8.3) and 1.25 units of Ampli Taq Gold polymerase (Applied Biosystems) was incubated at 25°C for 10 min, transcripted at 48°C for 30 min, and terminated by heating at 95°C for 5 min. PCR was performed in a 10-$\mu$L reaction volume using Kv 1.4 and Kv 4.1–4.3 gene expression assay kits and a standard TaqMan Universal PCR master mix with an initial denaturalization step at 95°C for 12 min followed by 50 cycles of amplication. Each cycle consisted of a denaturalization step at 94°C for 30 seconds, an annealing step at 65°C for 15 seconds, and an elongation step at 72°C for 15 seconds. The cycles were followed by a final elongation step at 72°C for 5 min. Concerning the expression of both Kv 1.4 and Kv 4 family amplifications were performed using the technique of an initial denaturalization step at 95°C for 2 min, followed by 35 cycles at 94°C for 15 seconds, 55°C for 30 seconds, and 72°C for 15 seconds. The PCR products were then separated on a 1.5% agarose gel stained with SYBR Green I (Invitrogen™ Life Technologies Japan Ltd., Tokyo, Japan).

## Immunoreactivity

The chests of four anesthetized rats, under artificial ventilation, were opened widely at the mid-section. The animals were transcardially perfused with a fixative, consisting of 100 mL of 4% paraformaldehyde in a 0.01 M phosphate buffer (PB, pH = 7.3) after perfusion with 50 mL heparinized saline in 0.01 M PB. The nodose ganglia were removed and stored with the same solution for 1 h; immersed in 4%, 10%, 20%, and 30% sucrose solutions (5 min × 3 times, 1 h, 3 h, and overnight, respectively) and embedded in an O.C.T. compound (Sakura Finetechnical, Tokyo, Japan); and then frozen. Subsequently, they were serially sectioned at a thickness of 10–15 $\mu$m on a cryostat (CM3050s, Leica Biosystem, Nussloch GmbH, Nussloch, Germany) to maintain a similar distribution of cells to be examined. Six serial sections in NG were washed in PB solution (PBS) for 5 min and nonspecific immunoreactivity was inhibited by 0.3% Triton X-100, 8% bovine serum albumin (Wako Pure Chemical Industries Ltd., Osaka, Japan) and 10% goat serum albumin (Wako Pure Chemical Industries Ltd., Osaka, Japan) in PBS for 60–90 min at room temperature. In order to demonstrate Kv 1.4 and CA-II, Kv 4.1 and CA-II, Kv 4.2 and CA-II, and Kv 4.3 and CA-II fluorescent double stainings, sections were separately exposed for a period of 2 days to mix the first antibody solution with rabbit anti-Kv 1.4 (1:160, Alomone Labs Ltd., Jerusalem, Israel) and sheep anti-CA-II polyclonal (1:500, Biogenesis, USA), rabbit anti-Kv 4.1 (1:160, Alomone Labs Ltd., Jerusalem) and sheep anti-CA-II polyclonal (1:500, Biogenesis), rabbit anti-Kv 4.2 (1:160, Chemicon) and sheep anti-CA-II polyclonal (1:500, Biogenesis) and rabbit anti-Kv 4.3 (1:160, Alomone Labs Ltd., Jerusalem) and sheep anti-CA-II polyclonal (1:500, Biogenesis) at 4°C followed by incubation in a secondary antibody solution with Alexa® 568 goat anti-rabbit IgG (1:1000, Molecular Probes, Kv 1.4, Kv 4.1–4.3, red, USA) and donkey anti IgG sheep-FITC (1:1000, CA-II, green, Chemicon) for 24 h at room temperature, respectively. After the sections were rinsed in PBS (5 min × 2 times), the samples were mounted using an anti-fade mounting medium (Molecular Probes). Control experiments were performed without the first antibody. Under control conditions, the section without the first antibody did not show any

immunoreactivity. We determined whether NG neurons express Kv 1.4, Kv 4.1–4.3, and CA-II immunoreactivities by comparison with the background activity for each antibody. The neurons with the most intense staining after subtraction of the control reaction were considered positive. The immunofluorescence was visualized using the appropriate filters. Digital images were collected and stored on a laboratory computer and later analyzed with Adobe Photoshop ver. 7.0 and a Leica Imaging Analysis Tool. Confocal images were generated using a Leica TCS SP laser scanning microscope (Leica, Microsystems CMC GmbH, Mannheim, Germany).

## Results

### Effects of AZ on $I_A$

The $K^+$ currents were recorded for medium and small NG neurons (<35 $\mu$m). We initially confirmed both the increased discharge rate and the increased resting membrane potential (RMP) in those neurons, having a response to the 1 mM AZ application and showing a slowly adapting (SA) type. Such neurons were observed in 65% of the NG neurons (a total of 31) recorded (Figure 1A). As shown in Figure 1B, we separated the $K^+$ currents according to their responses to variations in conditioning and identified two distinct components of voltage-gated $K^+$ currents, such as total outward $K^+$ current and sustained $K^+$ current ($I_K$). The neurons were first held at −60 mV, and were then increased to either −120 mV (Figure 1B, top and right panel) or −40 mV (Figure 1B, middle and right panel) for 300 ms (conditioning prepulse potentials, top and bottom left panels). We then depolarized the membrane potentials from −120 or −40 mV to +60 mV in increments of 10 mV. The transient $K^+$ current ($I_A$) was obtained by subtracting $I_K$ from the total outward $K^+$ current (Figure 1B, bottom and right panel). Before the application of 1 mM AZ, Figure 1C (left panel) showed the control $I_A$. The application of 1 mM AZ decreased $I_A$ (Figure 1C, middle panel) and 10 min following the end of the application, the decreased $I_A$ returned to the control level (Figure 1C, right panel). Such an inhibitory effect of 1 mM AZ on $I_A$ was seen in all 6 NG neurons examined. The peak values for $I_A$ before and after 1 mM AZ application and during recovery were 1.7 ± 0.1 nA, 1.3 ± 0.1 nA, and 1.6 ± 0.1 nA, respectively. In the peak current density–voltage relationship of $I_A$, the magnitude of decreased $I_A$ seen after 1 mM AZ application was 25.1 ± 5.5% ($P < 0.05$ vs. control, n = 6), and 10 min after ending the 1 mM AZ application, the $I_A$ tended to return to the control level (5.5 ± 1.0% inhibition of control $I_A$, $P < 0.05$ vs. AZ effect) (Figure 1D and E). In addition, we examined the effects of AZ at different concentrations (0.01, 0.1, 1, and 10 mM)

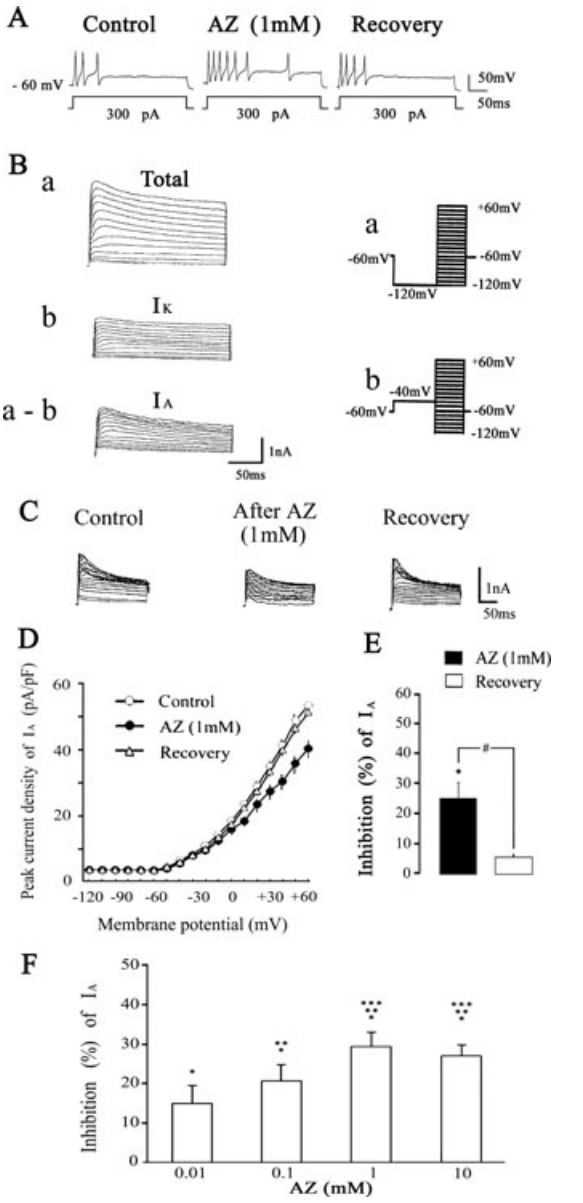


**Figure 1** Identification of NG neurons and effect of AZ on $I_A$. (**A**) Action potentials at 3T current injection before and after 1 mM AZ application as well as during recovery period. (**B**) Typical examples of three outward voltage-gated $K^+$ currents (total, $I_K$, and $I_A$). $I_A$ (a–b) was determined by subtraction of $I_K$ (b) from the total outward $K^+$ current (a). Right panels, voltage-pulse protocols (a and b). (**C**) Typical changes in $I_A$ before (control) and after the application of 1 mM AZ as well as during the recovery from AZ application. (**D**) Normalized I-V curves of $I_A$ were obtained before (○) and after (●) 1 mM AZ application as well as during the recovery from AZ application (△). (**E**) Baseline percent inhibition of $I_A$ seen after 1 mM AZ application (■) as well as during the recovery from AZ application (□). Each column represents the mean ± SEM. (n = 6). *Control versus AZ, #AZ versus Recovery. *,# $P < 0.05$. (**F**) Summary of AZ (0.01 0.1, 1 and 10 mM) inhibitory effects on $I_A$ in other groups of eight cells. Each column represents the mean ± SEM. (n = 8). *Control versus AZ (0.01, 0.1, 1, and 10 mM), **AZ (0.01 mM) versus AZ (0.1, 1, and 10 mM), ***AZ (0.1 mM) versus AZ (1 and 10 mM). *,**,***$P < 0.05$.

on the $I_A$. As shown in Figure 1F, the application of AZ concentration-dependently inhibited $I_A$. At a +60 mV step pulse, 0.01, 0.1, 1, and 10 mM AZ inhibited 14.7 ± 4.9% ($P < 0.05$ vs. control), 21.0 ± 3.9% ($P < 0.05$ vs. control and 0.01 mM AZ effect), and 29.6 ± 3.2% ($P < 0.05$ vs. control and 0.01 and 0.1 mM AZ effects), and 27.5 ± 2.4% ($P < 0.05$ vs. control and 0.01 and 0.1 mM effects) of the baseline $I_A$, respectively. Furthermore, AZ application at 1 mM caused a maximal decrease in the $I_A$.

## Effects of AZ and 4-AP on $I_A$

The $K^+$ current recordings were examined before and after AZ application (1 mM) in the absence and presence of 4-AP (1 mM). The typical effect of 4-AP (1 mM) on $I_A$ is also shown in Figure 2A. $I_A$ was relatively sensitive to 4-AP. The summarized results of the peak current density–voltage relationship of $I_A$ in the seven cell are shown in Figure 2B. The $I_A$ was significantly inhibited by the application of 1 mM 4-AP (47.6 ± 4.8%) only. To determine whether the AZ (1 mM)-induced inhibition $I_A$ is a subcomponent of the 4-AP (1 mM) effect, we also examined the changes in $I_A$ in response to 1 mM AZ application in the absence and presence of 4-AP (1 mM) on $I_A$ in the other group (Figure 2C). After the 1 mM AZ application, the $I_A$ was reduced. The $I_A$ was further reduced after co-application with 1 mM AZ plus 1 mM 4-AP. The summarized results of the peak current density–voltage relationship of $I_A$ of seven cells are shown in Figure 2D

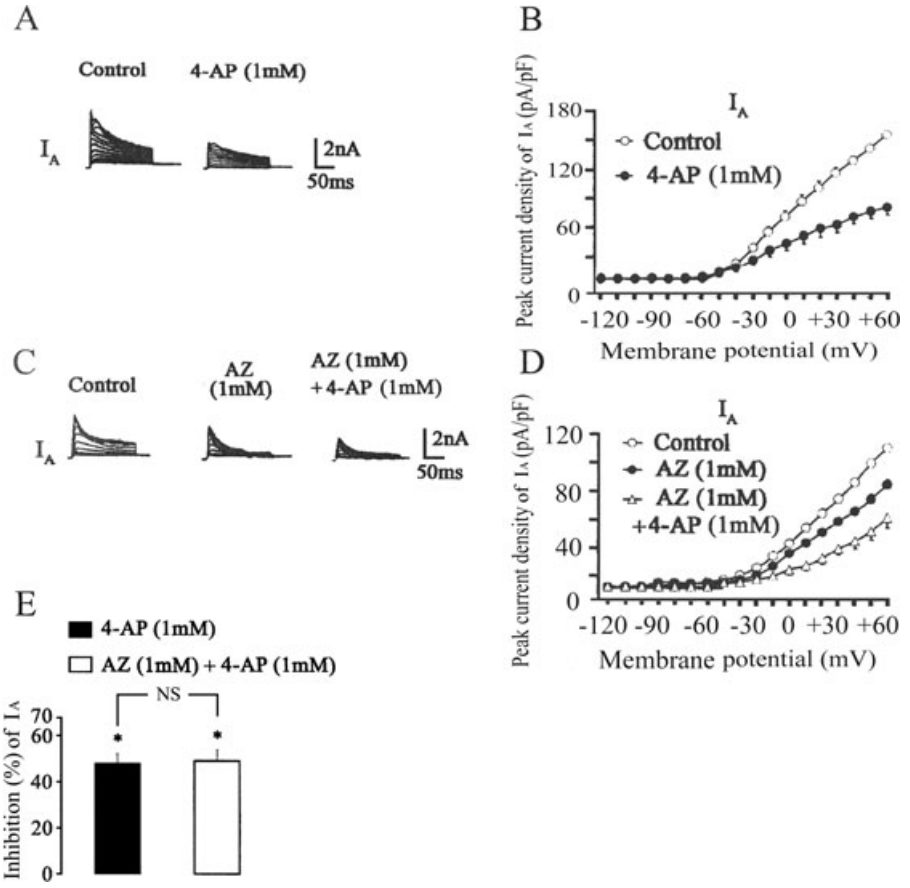


**Figure 2** Effects of 4-AP on $I_A$ in the absence or presence of AZ. (**A**) Typical changes in $I_A$ in response to 1 mM 4-AP application. (**B**) Normalized I-V curves of $I_A$ were obtained before (○, control) and after (●) 1 mM 4-AP application. (**C**) Typical changes in $I_A$ in response to 1 mM 4-AP application before and after 1 mM AZ in a different cell of another group. (**D**) Normalized I-V curves of $I_A$ before (○, control) and after the application of 1 mM 4-AP in the absence (●) and presence (△) of 1 mM AZ in other group. (**E**) Baseline percent inhibition of $I_A$ seen after 1 mM 4-AP application (■) only as well as co-application of 1 mM AZ and 1 mM 4-AP (□) in other group. Each column represents the mean ± SEM. (n = 6). *Control versus 4-AP, *Control versus 4-AP + AZ. *$P < 0.05$. NS, there were no significant differences in the inhibition (%) $I_A$ between 4-AP (1 mM) and AZ (1 mM) plus 4-AP (1 mM).

and E. At a +60 mV step pulse, $I_A$ was significantly inhibited by the application of 1 mM AZ (26.3 ± 2.9%), and the subsequent additional application of 1 mM 4-AP in the presence of 1 mM AZ resulted in a further inhibition of $I_A$ (48.1 ± 5.7%, $P < 0.05$ relative to the 1 mM AZ effects). As shown in Figure 2E, in different groups of the seven respective cells, the magnitude to which $I_A$ was inhibited after application of both AZ (1 mM) and 4-AP (1 mM) was similar to that after application of 1 mM 4-AP only.

## Effects of AZ and α-DTX on $I_A$

Since the maximal concentration of α-DTX to inhibit $I_D$ is 0.1 μM in rat TTX-R TG neurons [16], we used the same concentration of the D-current blocker. Figure 3A shows the effect of α-DTX (0.1 μM) on $I_A$. Three minutes after the application of 0.1 μM α-DTX, the $I_D$ was inhibited. The application of 0.1 μM α-DTX to seven cells significantly inhibited the $I_A$ at a +60 mV step pulse (Figure 3B). Figure 3C illustrates a typical example of the

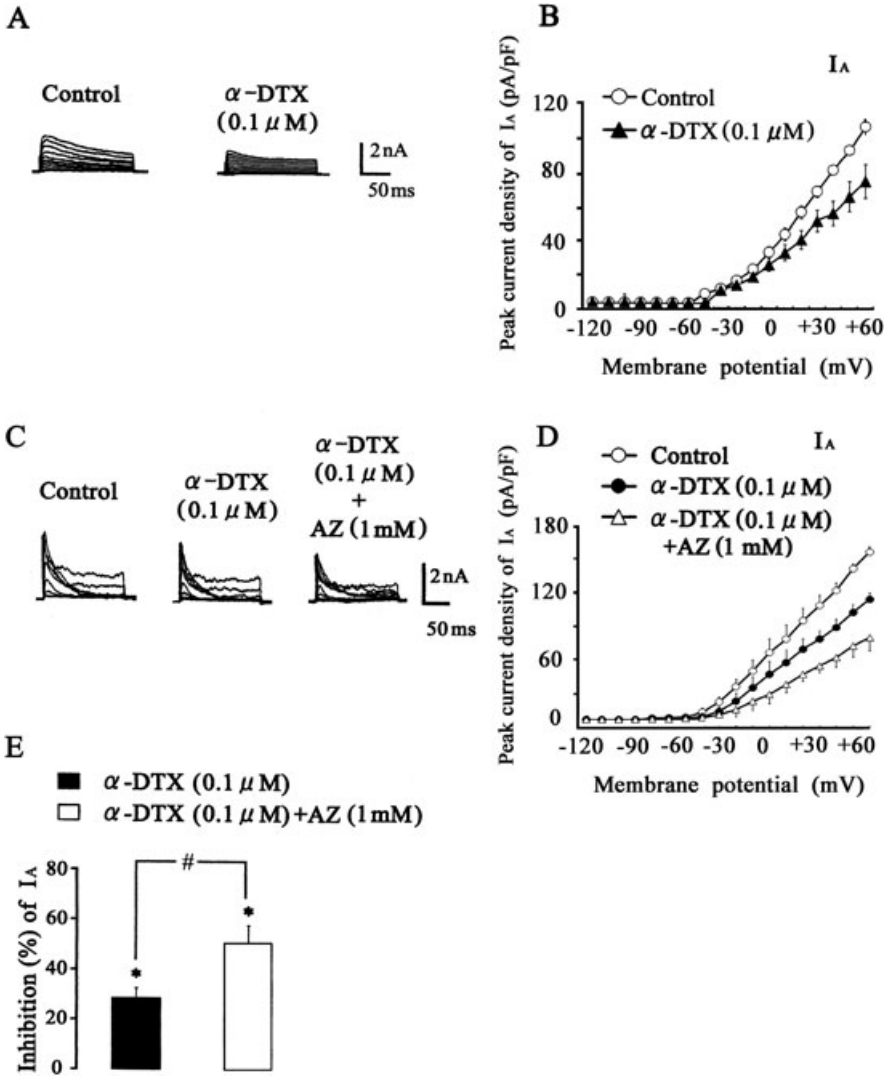


**Figure 3** Effects of α-DTX on $I_A$ in the absence or presence of AZ. (**A**) Typical changes in $I_A$ in response to 0.1 μM α-DTX application. (**B**) Normalized I-V curves of $I_A$ before (○, control) and after (●) 0.1 μM α-DTX application. (**C**) Typical changes in $I_A$ in response to 0.1 μM α-DTX application before and after 1 mM in a different cell of another group. (**D**) Normalized I-V curves of $I_A$ before (○, control) and after the application of 0.1 μM α-DTX in the absence (●) and presence (△) of 1 mM AZ in other group. (**E**) Baseline percent inhibition of $I_A$ seen after 0.1 μM α-DTX application (■) only as well as co-application of 0.1 μM α-DTX and 1 mM AZ (□) in other group. Each column represents the mean ± SEM (n = 6). *Control versus α-DTX, *Control versus α-DTX +AZ. #α-DTX versus α-DTX +AZ. $^{*,\#}P < 0.05$.

effects of application of $\alpha$-DTX (0.1 $\mu$M) in the absence and presence of AZ (1 mM) on $I_A$ in the other group. The $I_A$ was attenuated by application of 0.1 $\mu$M $\alpha$-DTX and further reduced after the additional application of 0.1 $\mu$M $\alpha$-DTX and 1 mM AZ (Figure 3D). The summarized results from two different groups of five respective cells are shown in Figure 3E. The magnitude of $I_A$ inhibition provoked by 0.1 $\mu$M $\alpha$-DTX only was 27.2 $\pm$ 4.5%. The $I_A$ in the other group of seven cells was significantly inhibited by application of 0.1 $\mu$M $\alpha$-DTX only (26.2 $\pm$ 4.0%), and the subsequent additional application of 1 mM AZ caused a further enhancement of the $\alpha$-DTX application-induced $I_A$ inhibition (51.1 $\pm$ 5.8%). In two different groups with or without the 1 mM AZ application, the inhibitory effects of $\alpha$-DTX on $I_A$ were almost the same. This implies that additional inhibition of $I_A$ seen after AZ application in the presence of $\alpha$-DTX is not involved in the contribution of $I_D$.

### Effects of AZ and 4-AP on Action Potentials

To determine whether the 1 mM AZ-induced inhibition of $I_A$ modulates the responses of NG neuronal activity, shown to be those of the SA type, to 3T current injection (300 pA), we examined changes in the neuronal activity in response to AZ (1 mM) application in the absence and presence of 4-AP (1 mM). During the depolarizing step pulse, as shown in Figure 4A, the NG neuron fired repeatedly and this neuron showed a SA type of firing pattern. AZ application (1 mM) increased the firing rates and increased the RMP level, and the subsequent additional application of 1 mM 4-AP further accelerated these two responses. The results from the seven cells are summarized in Figure 4B–F. The application of 1 mM AZ effectively increased the action potential number (2.7 $\pm$ 0.6 imp/s vs. 3.9 $\pm$ 0.6 imp/s, $P < 0.05$, Figure 4B), resulting in the reduction of the duration of the depolarizing phase of the action potential (DDP) (7.0 $\pm$ 1.2 ms vs. 5.4 $\pm$ 1.0 ms, $P < 0.05$, Figure 4D), and increased the RMP ($-58.3 \pm 2.4$ mV vs. $-48.9 \pm 1.7$ mV, $P < 0.05$, Figure 4C). The AZ-induced increase in the action potential number was significantly potentiated by the additional application of 4-AP (3.9 $\pm$ 0.6 imp/s vs. 5.2 $\pm$ 1.4 imp/s, $P < 0.05$, Figure 4B). The AZ-induced increase in the RMP was significantly enhanced by the additional application of 1 mM 4-AP ($-48.9 \pm 1.7$ mV vs. $-42.9 \pm 1.5$ mV, $P < 0.05$, Figure 4C). Furthermore, the duration of the repolarization phase of the action potential (DRP) was significantly prolonged by the additional application of 1 mM 4-AP in the continuous presence of 1 mM AZ (6.2 $\pm$ 0.4 ms or 6.6 $\pm$ 0.5 ms vs. 8.0 $\pm$ 0.4 ms; $P < 0.05$ vs. control or AZ effect, Figure 4E). The additional application of 1 mM 4-AP in the continuous presence of 1 mM AZ significantly increased the duration of the half-amplitude of the action potential (6.2 $\pm$ 0.7 ms or 6.1 $\pm$ 0.9 ms vs. 9.0 $\pm$ 0.2 ms; $P < 0.05$ vs. control or AZ effect, Figure 4F).

### The mRNA Expression of Kv 1.4 and the Kv 4 Family

The expression of both Kv 1.4 and the Kv 4 family (Kv 4.1–4.3) in the adult rat nodose ganglia was examined using the RT-PCR technique. mRNA was isolated from the nodose ganglia of six adult rats, and PCR was performed with the primers described in the Methods section. The primers selectively amplified mRNA fragments of the expected sizes for Kv 1.4 (b), Kv 4.1 (c), Kv 4.2 (d), Kv 4.3 (e), and GAPDH (f), as shown in Figure 5. The control sample that lacked the RT enzyme was negative, indicating that mRNA was not transcribed from genomic DNA (Figure 5g).

### Double Stainings for the Kv 1.4- or the Kv Family- (Kv 4.1–4.3) and CA-II-Immunoreactive Neurons

As shown in Figure 6, NG neurons showed immunoreactivity for Kv 1.4 (486/724, 67.1%), Kv 4.1 (449/728, 61.7%), Kv 4.2 (498/758, 65.7%), and Kv 4.3 (462/722, 64.0%). Furthermore, CA-II was co-expressed in neurons immunoreactive for Kv 1.4 (422/486, 86.5%), Kv 4.1 (404/449, 90.0%), Kv 4.2 (430/498, 86.3%), and Kv 4.3 (363/462, 78.6%) immunoreactive neurons. In this study, we classified NG cell bodies by size as small ($< 30$ $\mu$m), medium (30–40 $\mu$m), and large ($>40$ $\mu$m). There were few large NG neurons. All small-to-medium CA-II-immunoreactive neurons were also immunoreactive for both the Kv 1.4 and the Kv 4 family.

## Discussion

The present study provides evidence that the effect of AZ on the $K^+$ current is mediated by the inhibition of $I_A$ without affecting $I_D$ in adult rat NG neurons and that the response was associated with an increase in the action potential number via an increase in the RMP as well as a decrease in the DDP. Furthermore, we obtained that mRNAs for voltage-gated $K^+$ channels, Kv 1.4 and Kv 4.1–4.3, were identified by RT-PCR from rat NG, and that the immunoreactivity for four respective Kv channel proteins was co-expressed with that for CA-II. These results indicate that the excitability of adult rat NG neuronal activity seen after AZ application would occurs as a result of the inhibition of Kv families (Kv 1.4 and Kv 4.1–4.3).

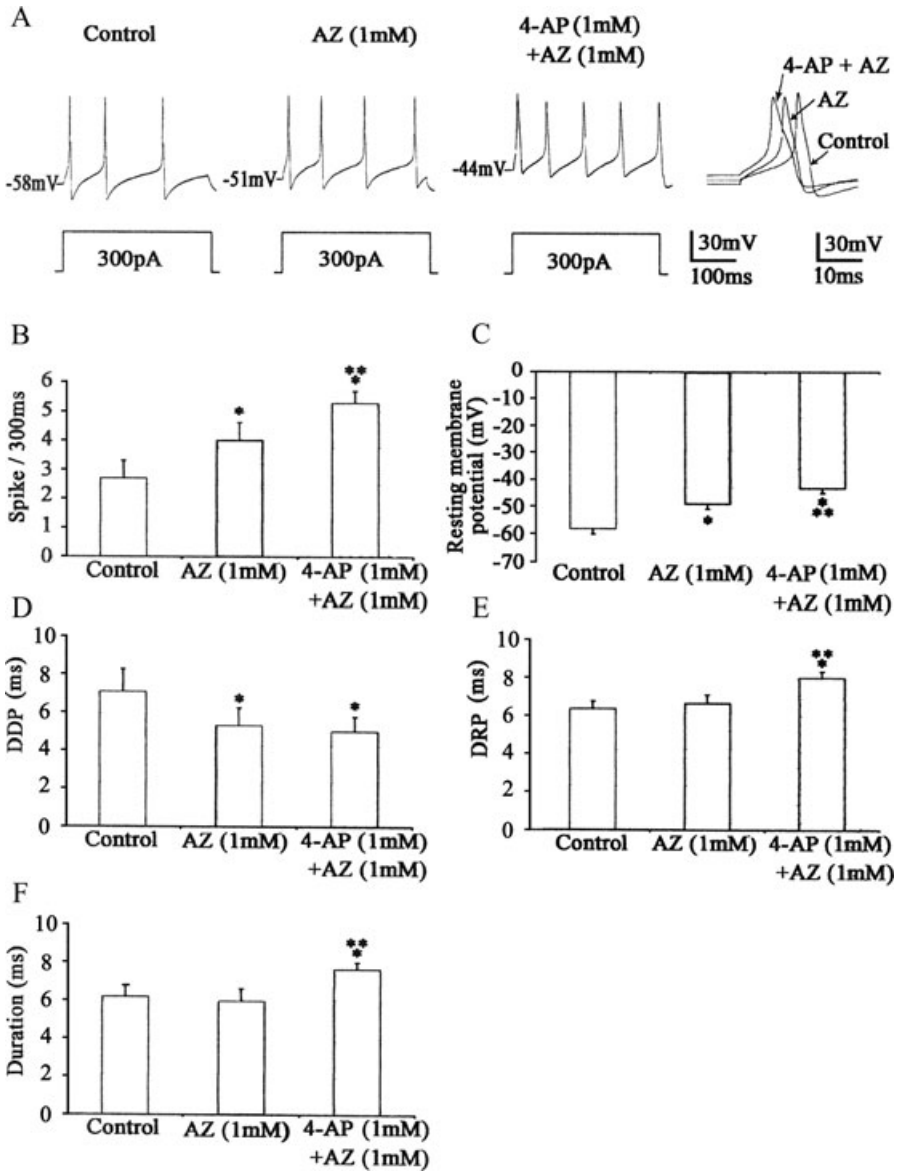


**Figure 4** Effects of AZ on the responses of slowly adapting type NG neurons to current injections before and after 4-AP. (**A**) Action potentials were induced by a 3 T current injection (300 pA) before and after 1 mM AZ application in the absence and presence of 1 mM 4-AP. Right panel, first action potentials before (control) and after AZ (1 mM) as well as after AZ (1 mM) plus 4-AP (1 mM). Changes in the number of spikes (**B**), resting membrane potential (**C**), DDP (**D**), DRP (**E**), and duration (**F**, duration of half-amplitude of action potential) in response to AZ (1 mM) in the absence and presence of 4-AP (1 mM). Each column represents the mean ± SEM. (n = 6). *Control versus AZ, *Control versus AZ+4-AP. **AZ versus AZ+4-AP. *·**$P < 0.05$.

The DRG and TG neurons contain three different types of $K^+$ currents in varying quantities: $I_K$, $I_A$, and $I_D$ [16,17,23,25,32–34]. In rat DRG neurons, Everill et al. [35] dentified three different combination of $K^+$ currents (A, K, and D currents, A and K currents, and K and D currents) in the population of cells examined. Such a classification is very similar to $I_A$, $I_D$, and $I_K$, as reported by McFarlane and Cooper [9] in neonatal rat NG neurons. A-type Kv channels in sensory neurons involve Kv families, such as Kv 1.4 and Kv 4.1–4.3 [36,37]. The fact that in the medium-and small-sized (A$\delta$- and C-) nociceptive DRG neurons the reduction in Kv 1.4 occurred after the sciatic nerve injury [36] and that the tempromandibular joint (TMJ) inflammation decreased the expression of Kv 1.4 subunits in A$\delta$- and C-type TG neurons [38] suggests that homogenetic Kv 1.4 channels are

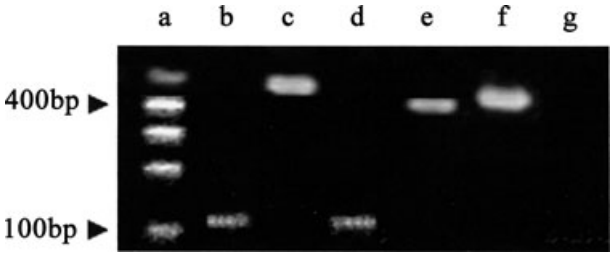


**Figure 5** Example of mRNA encoding Kv 1.4 and Kv 4 family channel proteins in adult rat nodose ganglia. Gel electrophoresis of PCR products obtained from nodose ganglia. **a**), A nucleotide size ladder in 100 bp increments. PCR products obtained with the primer for Kv 1.4 (119 bp, **b**), Kv 4.1 (467 bp, **c**), Kv 4.2 (110 bp, **d**), Kv 4.3 (400 bp, **e**), and GAPDH (418 bp, **f**). Negative control (no reverse transcription, **g**).

predominant on A$\delta$- and C-type axons. However, it has been reported that the mRNA encodings for the Kv 4 family (Kv 4.1–4.3) are present in the rat dorsal root ganglia [37]. In addition, 4-AP application significantly reduces the latency of firing and increases the action potential number in isolectin $B_4$-positive DRG neurons immunoreactive to Kv 1.4 but not to Kv 1.1 and Kv 1.2 subunits [37]. Tanimoto et al. [39] demonstrated that small-diameter Kv 1.4 positive TG neurons also co-expressed CA-II immunoreactivity. In the present study, the gene protein expression of four Kv channels (Kv 1.4 and Kv 4.1–4.3) was found in the nodose ganglia. Furthermore, we found that 80–90% of the CA-II immunoreactive neurons (12–46 $\mu$m, in diameter) examined were also immunoreactive to either Kv 1.4 or the Kv 4 family of channel proteins. Therefore, it is possible to speculate that the AZ effect on the CA-II activity of NG neurons resembles the blocking action of the A-type currents represented by Kv 1.4 and Kv 4.1–4.3 channel subunits.

Maren [29] demonstrated that a 20 mg/kg dose of AZ inhibited 99.99% of the CA enzyme. For the applications of AZ, ranging from 0.01 to 10 mM, the 1 mM AZ application showed a maximal inhibition of $I_A$. The magnitude of reduced $I_A$ was approximately 27% in the four different groups (AZ at 1 mM, AZ at 0.01–10 mM, 1 mM 4-AP+1 mM AZ, and 0.1 $\mu$M $\alpha$-DTX+1 mM AZ).

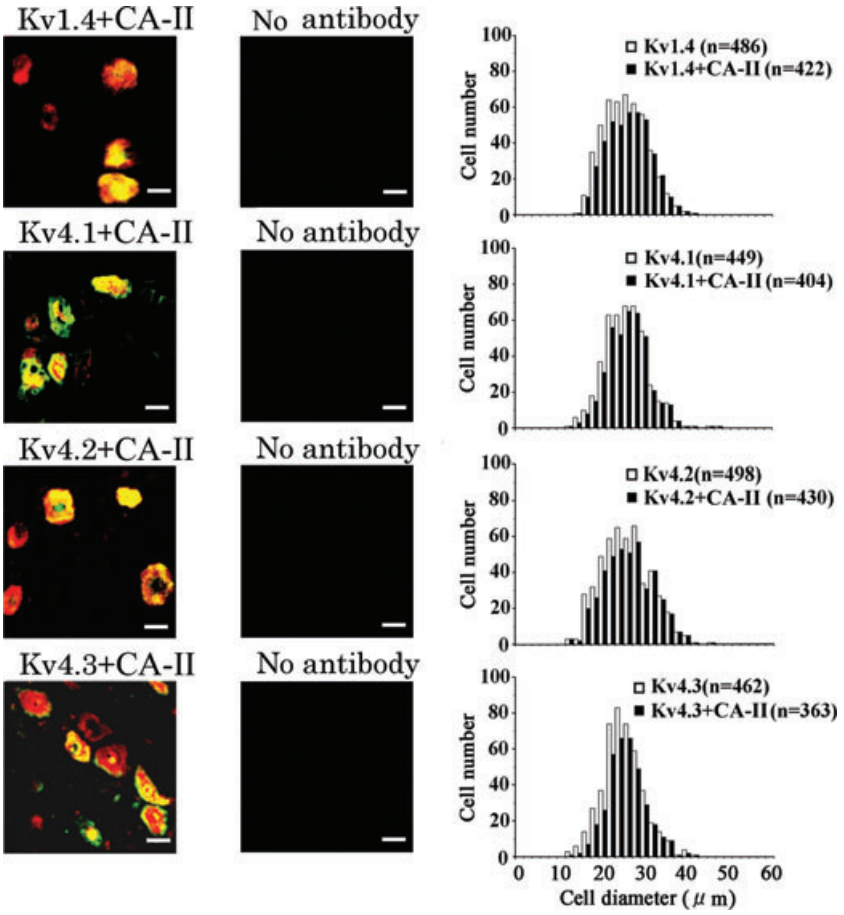


**Figure 6** Immunofluorescence staining of adult rat nodose ganglion neurons and histograms showing diameters of cells labeled with four Kv channel (Kv 1.4, Kv 4.1–4.3) and/or CA-II antibodies. Scale bars are 20 $\mu$m.

Therefore, it is most likely that the concentration of 1 mM AZ used reflects the inhibition of CA-II activity of adult rat NG neurons.

The SAR afferent and/or many myelinated fibers are not activated by capsaicin, a selective agonist of the transient receptor potential vanilloid type 1 (TRPV1) receptors [40,41]. This probably implies that capsaicin may be a useful tool for identifying the soma of SARs. However, there is evidence that myelinated capsaicin-sensitive nociceptive lung afferents exist in guinea-pig lungs [42]. Furthermore, TRPV1 receptors are also expressed in approximately 30% of myelinated fibers in the somatic nerve fibers [43]. Sun et al. [44] have recently demonstrated that TRPV1 receptors are expressed in a small number of aortic baroreceptor afferents, consisting of myelinated fibers. The application of the TRPV1 receptor antagonist, capsazepine, can prevent constriction of human small airways in *in vitro* experiments [45,46]. If NG neurons are capsaicin insensitive, this criterion would narrow to identify a class of the neurons that include SARs. Furthermore, Kwong et al. [42] reported that in electrophysiological studies, gene expression studies, and immunohistochemical observations, the tetrodotoxin-resistant (TTX-R) $Na^+$ channels were similarly distributed between NG A-fibers and C-fibers innervating the lungs. The results indicate that some medium-sized NG neurons are insensitive to TTX. The SARs are well known to be one of the mechanoreceptors in the lung. Taken together, the fact that most NG neurons have unmyelinated fibers or that NG neurons innervate many viscera other than the airways, it would be difficult to accurately define whether the NG neurons recorded are the soma of SARs.

AZ is known to block reabsorption of sodium bicarbonate and to inhibit $H^+$ secretion by the renal tubule [47]. Regarding the cerebral circulation, AZ has a vaso-relaxant action on the blood vessels [48,49]. The administration of AZ stimulates large conductance $Ca^{2+}$-activated $K^+$ (BK) channels to alter human forearm vascular tone in *in vivo* experiments [50], and also prevents vacuolar myopathy in $K^+$-depleted rats [51]. Furthermore, AZ treatment can weaken the development of acute mountain sickness, resulting in the renal bicarbonate reabsorption as well as a decrease in overall hypoxic sensitivity due to the inhibition of the carotid chemoreceptor-induced ventilatory reflex [52,53]. Additionally, abnormal levels of $K^+$ associated with skeletal muscle disorder are observed in AZ-responsive periodic paralysis [54–56]. From these observations, it is possible to speculate that the different pharmacological effects of AZ are due to the ubiquitous distribution of CA within the body because the enzyme plays an important role in so many physiological functions [29,57]. Further studies are needed to determine whether those effects of AZ, as described above, are involved in the one characteristic of the CA inhibitor that inhibits $I_A$ in adult rat NG neurons selectively.

The application of 1 mM 4-AP, which was a concentration (ranging from 0.05 to 50 mM) nearly equal to the $IC_{50}$ value in adult rat TTX-R TG neurons [22], caused approximately 50% inhibition of the $I_A$, irrespective of the absence and presence of 1 mM AZ. Since the efficiency of AZ on the inhibition of $I_A$ was almost the same for all four of the four different experimental conditions, the 4-AP (1 mM)-induced $I_A$ inhibition could be divided into AZ-sensitive and AZ-insensitive components. The results of this study lead us to suggest that after the blockade of 1 mM AZ on $I_A$, the remaining 4-AP-sensitive $K^+$ currents are still active in medium and small NG neurons.

It has been reported that the D current is different from $I_A$, showing greater sensitivity to lower concentrations of $\alpha$-DTX (0.001–1 $\mu$M) and 4-AP (50–500 $\mu$M) in DRG and TG neurons [15,16,23]. Alpha-DTX $K^+$ currents were expressed by Kv 1.1, Kv 1.2, and Kv 1.6 in adult rat NG neurons [15]. In adult rat TTX-R TG neurons, maximal blockade of $I_D$ by $\alpha$-DTX was 0.1 $\mu$M [16]. Furthermore, the selective blockade of $I_D$ by $\alpha$-DTX was 0.01–0.1 $\mu$M in neonatal rat TTX-R NG neurons [15]. Although the $I_D$ has the ability to delay the firing rates after a depolarizing current step and is sensitive to lower concentrations of $\alpha$- DTX and 4-AP [14,16], the inhibition of $I_A$ evoked by 0.1 $\mu$M $\alpha$-DTX application was approximately 20%, irrespective of the absence and presence of 0.5 mM 4-AP [16]. The present study showed that the inhibition of $I_A$ seen after 0.1 $\mu$M $\alpha$-DTX application was approximately 27%, irrespective of the absence or presence of 1 mM 4-AP. This probably implies that the component of $I_D$ in the NG neurons may be larger than that in the TG neurons. Furthermore, we obtained evidence that the additional application of 1 mM AZ significantly inhibited $I_A$ to a greater extent than the 0.1 $\mu$M $\alpha$-DTX application alone. Considering the fact that $I_A$ in the presence of 0.1 $\mu$M $\alpha$-DTX application was further reduced by additional application of 1 mM AZ, we speculate that AZ has the potential to selectively block $I_A$, which is independent of the effect on $I_D$ in adult rat NG neurons.

In current-clamp experiments, 1 mM AZ application increased the RMP as well as the action potential number in a slowly adapting (SA) type of NG neurons. The latter effect was accompanied by a decrease in the DDP, indicating that the threshold for the first action potential was reduced by AZ application. This enhanced activity of SA type NG neurons was similarly manifested by increasing the threshold currents required to evoke action potentials in the absence of AZ. The application of both AZ (1 mM) and 4-AP (1 mM) caused a further increase in the action potential number, and the response was usually

associated with an elevation of the RMP in the first action potential and showed a significant increase in either the duration of the half-amplitude of the action potential or the DRP. In the study to determine whether there is a functional difference between $I_A$ and $I_K$ on the action potential in TTX-R adult rat TG neurons, irrespective of the absence and presence of TEA (2 mM, nearly equal to the $IC_{50}$ value), the application of 0.5 mM 4-AP (nearly equal to the $IC_{50}$ value) application increased the action potential number due to the reduction in the DDP. The response was associated with an elevation of the RMP, and the approximately 50% inhibition of $I_A$ seen after 1 mM 4-AP application was associated with the approximately 17% inhibition of $I_K$ [22]. This probably implies that the prolongation of both the half-amplitude duration and the DRP after the application of AZ (1 mM) combined with 1 mM 4-AP occurred as a result of the strong inhibition of $I_A$, partly involving the TEA-like effect. The fact that the RMPs were different across the depolarizing step pulses in the case of the AZ and/or 4-AP applications does not completely rule out the possibility concerning the contributions of either the gating probability or the voltage-dependence of TTX-sensitive (TTX-S) $Na^+$ channels. Further studies are needed to clarify the effect on the TTX-S $Na^+$ current in adult rat NG neurons. When considering the results of this study, taken together, it is conceivable that changes in action potential properties in response to 1 mM 4-AP application may consist of AZ (1 mM)-sensitive and -insensitive effects.

In conclusion, our results have demonstrated that the external application of 1 mM AZ in isolated NG neurons can decrease $I_A$. In addition, this decrease may be mediated by the inhibition of $I_A$, consisting of Kv 1.4 and Kv 4.1–4.3 channel subunits, but not by the inhibition of $I_D$. Finally, AZ has the effects of enhancing the intrinsic firing rates of the action potential in rat NG neurons of both small and medium sizes.

## Conflict of Interest

The authors state no conflict of interest.

### References


1. Stansfeld CE, Wallis DI. Properties of visceral primary afferent neurons in the nodose ganglion of the rabbit. *J Neurophysiol* 1985;**54**:245–260.
2. Undem BJ, Weinreich D. Electrophysiological properties and chemosensitivity of guinea pig nodose ganglion neurons *in vitro*. *J Auton Nerv Syst* 1993;**44**:17–33.
3. Li B-Y, Schild JH. Electrophysiological and pharmacological validation of vagal afferent fiber type of neurons enzymatically isolated from rat nodose ganglia. *J Neurosci Methods* 2007;**164**:75–85.
4. Matsumoto S, Okamura H, Suzuki K, Sugai N, Shimizu T. Inhibitory mechanism of $CO_2$ inhalation on slowly adapting pulmonary stretch receptors in the anesthetized rabbit. *J Pharmacol Exp Ther* 1998;**279**:402–409.
5. Matsumoto S, Takahashi T, Tanimoto T, Saiki C, Takeda M. Effects of potassium channel blockers on $CO_2$-induced slowly adapting pulmonarstretch receptor inhibition. *J Pharmacol Exp Ther* 1999;**290**:974–979.
6. Matsumoto S, Ikeda M, Nishikawa T, et al. Effects of acetazolamide and 4-aminoprydine on the responses of deflationary slowly adapting pulmonary stretch receptors to $CO_2$ inhalation in the rat. *Life Sci* 2003;**72**:1757–1771.
7. Matsumoto S, Tanimoto T, Yoshida S, et al. Effects of acetazolamide and 4-aminoprydine on $CO_2$-induced slowly adapting pulmonary stretch receptor inhibition in rats. *Chem Sences* 2004;**29**:351–361.
8. Higashi H, Ueda N, Nishi S, Gallagher JP, Shinnnick-Gallagher P. Chemoreceptors for serotonin (5-HT), acetylcholine (Ach), bradykinin (BK), histamine (H) and gamma-aminobutyric acid (GABA) on rabbit visceral afferent neurons. *Brain Res Bull* 1992;**8**:23–32.
9. McFarlane S, Cooper E. Kinetics and voltage dependence of A-type currents on neonatal rat sensory neurons. *J Neurophysiol* 1991;**66**:1380–1391.
10. Christian EP, Togo J, Naper KE. Guinei pig visceral C-fiber neurons are diverse with respect to the $K^+$ currents involved in action-potential repolarization. *J Neurophysiol* 1994;**71**:561–574.
11. Schild JH, Clark JW, Hay M, Mendelowitz D, Andresen MC, Kunze DL. A- and C-type rat nodose sensory neurons: Model interpretations of dynamic discharge characteristics. *J Neurophysiol* 1994;**71**:2338–2358.
12. Stansfeld CE, Mersh SJ, Halliwell JV, Brown DA. 4-aminoprydine and dendrotoxin induce repetitive firing in rat visceral sensory neurons by blocking a slow inactivating outward current. *Neurosci Lett* 1986;**64**:299–304.
13. Storm JF. Intracellular injection of a $Ca^{2+}$ chelator inhibits spike repolarization in hippocampal neurons. *Brain Res* 1987;**435**:387–392.
14. Coetzee WA, Amarillo Y, Chiu J, et al. Molecular diversity of $K^+$ channels. *Ann NY Acad Sci* 1999;**868**:233–285.
15. Glazebrook P, Ramirez AN, Schild JH, Shieh CC, Doan T, Wible BA, Kunze DL. Potassium channels Kv1.1, Kv1.2 and Kv1.6 influence excitability of rat visceral sensory neurons. *J Physiol* 2002;**541**:467–482.
16. Yoshida S, Matsumoto S. Effects of $\alpha$-dendrotoxin on $K^+$ currents and action potentials in tetrodotoxin-resistant adult rat trigeminal ganglion neurons. *J Pharmacol Exp Ther* 2005;**314**:437–445.
17. McAlexander MA, Undem BJ. Potassium channel blockade induces action potential generation in guinea-pig airway vagal afferent neurons. *J Auto Nerv Syst* 2000;**78**:158–164.

18. Harper AA. Similarities between some properties of the soma and sensory receptors of primary afferent neurons. *Exp Physiol* 1991;**76**:369–377.
19. Ikeda M, Yoshida S, Kadoi J, Nakano Y, Matsumoto S. The effect of PKC activity on the TTX-R sodium currents from rat nodose ganglion neurons. *Life Sci* 2005;**78**:47–53.
20. Matsumoto S, Ikeda M, Yoshida S, Tanimoto T, Takeda M, Nasu M. Prostaglandin $E_2$-induced modification of tetrodotoxin-resistant $Na^+$ currents involves activation of both $EP_2$ and $EP_4$ receptors in neonatal rat nodose ganglion neurons. *Br J Pharmacol* 2005;**145**:503–513.
21. Matsumoto S, Yoshida S, Ikeda M, et al. Effect of 8-bromo-cAMP on the tetrodotoxin-resistant sodium (Nav 1.8) current in small-diameter nodose ganglion neurons. *Neuropharmacology* 2007;**52**:904–92422.
22. Yoshida S, Takahashi M, Kadoi J, Kitagawa J, Saiki C, Takeda M, Matsumoto S. The functional difference between transient and sustained $K^+$ currents on the action potentials in tetrodotoxin-resistant adult rat trigeminal ganglion neurons. *Brain Res* 2007;**1152**:64–74.
23. Mo ZL, Davis RL. Endogenous firing patterns of murine spinal ganglion neurons. *J Neurophysiol* 1997;**77**:1294–1305.
24. Tsutsui Y, Ikeda M, Takeda M, Matsumoto S. Excitability of small-diameter trigeminal ganglion neurons by 5-HT is mediated by enhancement of the tetrodotoxin-resistant sodium current due to the activation of 5-$HT_4$ receptors and/or by the inhibition of the transient potassium current. *Neuroscience* 2008;**157**:683–696.
25. Gold MS, Shuster MJ, Levine JD. Characterization of six voltage-gated $K^+$ currents in adult rat sensory neurons. *J Neurophysiol* 1996;**75**:2629–2646.
26. Everill B, Kocsis JD. Reduction in potassium currents in identified cutaneous afferent dorsal root ganglion neurons after axotomy. *J Neurophysiol* 1999;**82**:700–708.
27. Takeda M, Tanimoto T, Ikeda M, Kadoi J, Matsumoto S. Activation of $GABA_B$ receptor inhibits the excitability of rat small diameter trigeminal root ganglion neurons. *Neuroscience* 2004;**123**:491–505.
28. Ikeda M, Matsumoto S. Classification of voltage-dependent $Ca^{2+}$ channels in trigeminal ganglion neurons from neonatal rats. *Life Sci* 2003;**73**:1175–1187.
29. Maren TH. Use of inhibitors in physiological studies of carbonic anhydrase. *Am J Physiol* 1977;**232**:F291–F297.
30. Lee HB, Blaufox MD. Blood volume in the rat. *J Neucl Med* 1985;**25**:72–76.
31. Wang EQ, Lee W-I, Brazeau D, Fung H-L. cDNA microarray analysis of vascular gene expression after nitric oxide donor infusion in rats: Implications for nitrate tolerance mechanisms. *AAPS Pharm Sci* 2002;**4**:1–11.
32. Puil E, Miura RM, Spigelman I. Consequence of 4-aminoprydine application to trigenal root ganglion neurons. *J Neurophysiol* 1989;**62**:810–820.
33. Everill B, Rizzo MA, Kocsis D. Morphologically identified cutaneous afferent DRG neurons express three different potassium currents in varying properties. *J Neurophysiol* 1998;**79**:1814–1824.
34. Seifert G, Kuprijanova E, Zhou M, Steinhäuser C. Developmental changes in the expression of Shaker- and Shab-related K(+) channels in neurons of the rat trigeminal ganglion. *Brain Res Mol Brain Res* 1999;**74**: 55–68.
35. Everill B, Rizzo MA, Kocsis JD. Morphologically identified cutaneous afferent DRG neurons express three different potassium currents in varying properties. *J Neurophysiol* 1998;**79**:1814–1824.
36. Rasband MN, Park EW, Vanderah TW, Lai J, Porreca F, Trimmer JS. Distinct potassium channels on pain-sensing neurons. *Proc Natl Acad Sci USA* 2001;**98**:13373–13378.
37. Winkelman DL, Beck CL, Ypey DL, O'Leary ME. Inhibition of the A-type $K^+$ channels of dorsal root ganglion neurons by the long-duration anesthetic butamben. *J Pharmacol Exp Ther* 2005;**314**:1177–1186.
38. Takeda M, Tanimoto T, Nasu M, Matsumoto S. Tempromandibular joint inflammation decreases the voltage-gated $K^+$ channel subtype 1.4-immunoreactivity of trigeminal ganglion neurons in rats. *Eur J Pain* 2008;**12**:189–195.
39. Tanimoto T, Takeda M, Nasu M, Matsumoto S. Immunohistochemical co-expression of carbonic anhydrase II with Kv 1.4 and TRPV1 in the rat small-diameter trigeminal ganglion neurons. *Brain Res* 2005;**1044**:262–265.
40. Ho CY, Gu Q, Lin YS, Lee L-Y. Sensitivity of vagal afferent endings to chemical irritants in rat lung. *Respir Physiol* 2001;**127**:113–124.
41. Zhang G, Lin R-Y, Wiggers M, Snow DM, Lee L-Y. Altered expression of TRPV1 and sensitivity to capsaicin in pulmonary myelinated afferents following chronic airway inflammation in the rat. *J Physiol* 2008;**586**:5771–5786.
42. Kwong K, Carr MJ, Gibbard A, et al. Voltage-gated sodium channels in nociceptive versus non-nociceptive nodode vagal sensory neurons innervating guines pig lungs. *J Physiol* 2008;**586**:1321–1336.
43. Ma QP. Expression of capsaicin receptor (VR1) by myelinated primary afferents neurons in the rat. *Neurosci Lett* 2002;**319**:87–90.
44. Sun H, Li H-P, Chen S-R, Hittelnan WN, Pan H-L. Sensory of blood pressure induced by transient receptor potential vanilloid 1 receptors on baroreceptors. *J Pharmacol Exp Ther* 2009;**331**:851–859.
45. Dalence-Guzman MF, Berglund M, Skogvall S, Sterner O. SAR studies of capsazepinoid bronchodilators. Part1: The importance of the catechol moiety and aspects of the B-ring structure. *Bioorg Med Chem* 2008;**16**:2499–2512.
46. Skogvall S, Berglund M, Dalence-Guzmán MF, Svensson K, Jönsson P, Persson CG, Sterner O. Effects of capsazepine on human small airway responsiveness unravel a novel class of bronchorelaxants. *Pulm Pharmacol Ther* 2007;**20**:273–280.

47. Hasannejad H, Takeda M, Taki K, et al. Interactions of human organic anion transporters with diuretics. *J Pharmacol Exp Ther* 2004;**308**:1021–1029.
48. Faraci FM, Mayhan WG, Heistad DD. Vascular effects of acetazolamide on the choroid plexus. *J Pharmacol Exp Ther* 1990;**254**:23–27.
49. Wang Q, Paulson OB, Lassen NA. Indomethacin abolishes cerebral blood flow increase in response to acetazolamide-induced extracellular acidosis: A mechanism for its effect on hypercapnia? *J Cereb Blood Flow Metab* 1993;**13**:724–727.
50. Pickkers P, Hughes AD, Russel FG, Thien T, Smits T. *In vivo* evidence for K(Ca) channel opening properties of acetazolamide in the human vasculature. *Br J Pharmacol* 2001;**132**:443–450.
51. Tricarico D, Lovaglio S, Mele A, Rotondo G, Mancinelli E, Meola G, Camerino DC. Acetazolamide prevents vacuolar myopathy in skeletal muscle of $K^+$-depleted rats. *Br J Pharmacol* 2008;**154**:183–190.
52. Swenson ER. Carbonic anhydrase inhibitors and ventilation: A complex interplay of stimulation and suppression. *Eur Respir J* 1998;**12**:1242–1247.
53. Teppema LJ, Dahan A. Low-dose acetazolamide reduces the hypoxic ventilatory response in the anesthetized cat. *Respir Physiol Neurobiol* 2004;**140**:43–51.
54. Lehmann-Horn F, Rüdel R, Jurkat-Rott K. In: Engel AG, Franzini-Armstrong C, editors. *Altered excitability of the cell membrane: Myology*, 3rd ed., vol. 46. USA: McGraw-Hill Press, 2004;1257–1300.
55. Clare BW, Supuran CT. A perspective on quantitative structure-activity relationships and carbonic anhydrase inhibitors. *Expert Opin Drug Metab Toxicol* 2006;**2**:113–137.
56. Venance SL, Cannon SC, Fialho D, et al. CINCH investigators. The primary periodic paralyses: Diagnosis, pathogenesis and treatment. *Brain* 2006;**129**:8–17.
57. Sly WS, Hu PY. Human carbonic anhydrases and carbonic anhydrase deficiencies. *Annu Rev Biochem* 1995;**64**:375–401.